Support information

Ultra-Strong, Recyclable, Self-Healable and Transparent Polythiourethane-Urea Elastomer via Physical-Chemical Dual-Reversible Networks Synergy

Yingxia Liang, Lin Li, Xun Lu*

Experimental Section

Feedstock Molar Ratios Detailed molar ratios of all reactants used in the synthesis of PUU and PTUU elastomers are provided in Table S1.

Table S1. Feeding molar ratios of the experimen

	PTMEG2000	HMDI	ID	DDM	PETMP
PUU-I$_9$D	1	2	0.9	0.1	0
PUU-I$_2$D	1	2	0.67	0.33	0
PUU-ID	1	2	0.5	0.5	0
PUU-ID$_2$	1	2	0.33	0.67	0
PUU-ID$_9$	1	2	0.1	0.9	0
PTUU-C$_1$	1	2.1	0.67	0.33	0.05
PTUU-C$_2$	1	2.15	0.67	0.33	0.075
PTUU-C$_3$	1	2.2	0.67	0.33	0.1

The decrosslinking mechanism of PTUU using 3 times the mass of PETMP is shown in Fig. S1; the red-marked parts are the thiocarbamate bonds in PTUU polymer chains that participate in an exchange reaction with free thiol groups from PETMP.

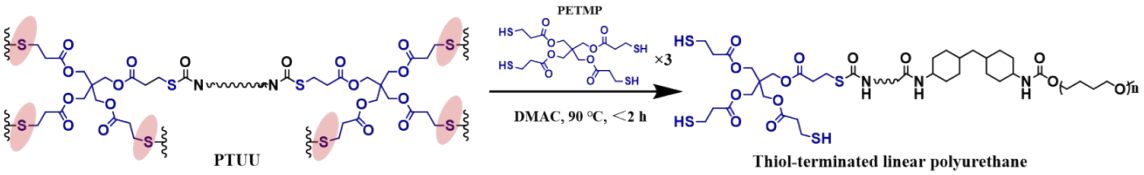

Figure S1. Decrosslinking mechanism of cross-linked elastomer PTUU

Instrumentation and Testing Methods A comprehensive list of instruments and corresponding test

methods is given in Table S2.

Table S2. Laboratory instruments and equipment

Instrument/Equipment Name	Model/Specification	Production/Sales Manufacturer
Fourier Transform Infrared Spectrometer	VERTEX 70v	Bruker, Germany
Universal Material Testing Machine	AGX-VD	Shimadzu, Japan
Universal Testing Machine	Instron 5966	Instron, USA
X-ray Diffractometer	XPer Pro MRD	PANalytical, Netherlands
Large Sample Scanning Probe Microscope	Bruker Icon	Bruker, Germany
UV-Vis Spectrophotometer	UV-2600i	Shimadzu, Japan
Fluorescence Spectrometer	Fluoromax PLUS R928P	HORIBA, Japan
Steady-State/Transient Fluorescence Spectrometer	FLS 1000	Edinburgh Instruments, UK
High Precision Crystallographic X-ray Diffractometer	CS-720	Hangzhou Colorful Spectroscopy Technology Co. Ltd.
Microdensitometer	2010M	Mettler Toledo, USA
Thermogravimetric Analyzer	TG 209 F3	Mettler Toledo, Switzerland
Dynamic Mechanical Analyzer	DMA-242E	Mettler Toledo, Switzerland
Dynamic Mechanical Thermal Analyzer	TA-Q800	TA Instruments, USA
Small Angle X-ray Scattering	Xenuss 2.0	Xenocs, France
Thermal Oxidation Chamber	GT7017-BM1	High Precision Testing Instruments (Dongguan) Co. Ltd.
600M Superconducting Nuclear Magnetic Resonance Spectrometer	AVANCE III HD 600	Bruker, Switzerland

Results and Discussion

XRD Analysis Wide-angle X-ray diffraction patterns (Fig. S2) confirm the amorphous structure of all elastomers.

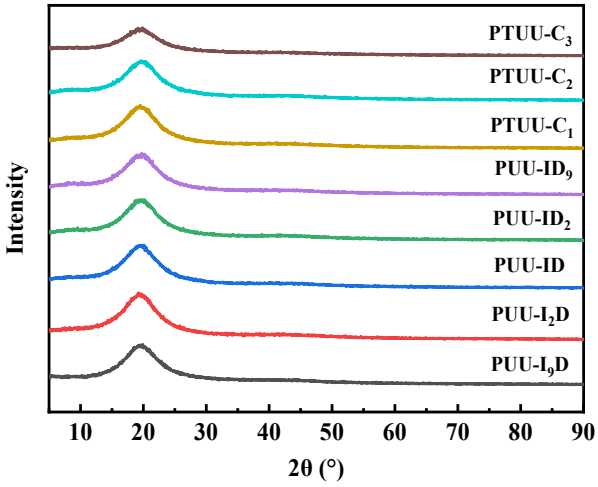

Figure S2. XRD curve of PUU and PTUU elastomers

Swelling Behavior Equilibrium swelling data and gel contents are summarized in Table S3.

Table S3. Swelling properties of PTUU elastomers

	PTUU-C_1	PTUU-C_2	PTUU-C_3
Average swelling rate/%	97	85	87
Average gel content/%	93	94	93

The results of the investigation on π-π stacking interactions by UV-Vis absorption spectroscopy and fluorescence emission spectroscopy are shown in Fig. S3.

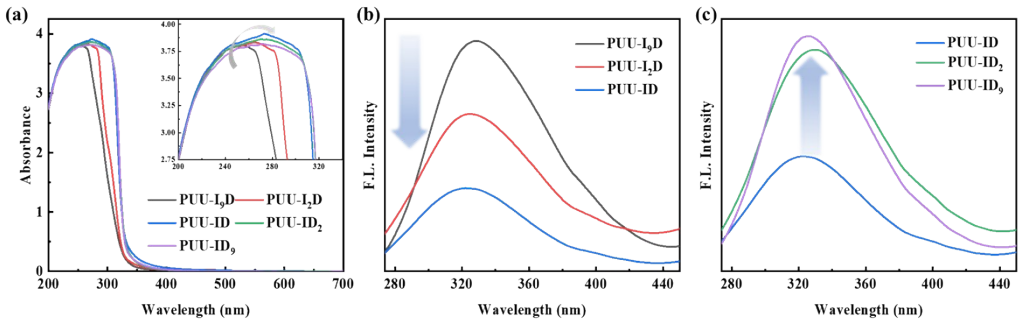

Figure S3. a)UV absorption spectra of PUU elastomers in the wavelength range of 200 ~ 700

nm. b)&c) fluorescence emission spectra of PUU elastomers in the wavelength range of 274 ~ 450 nm.

The curve-fitting results of FTIR spectra in the C=O stretching region for PUU and PTUU elastomers are shown in Fig. S4.

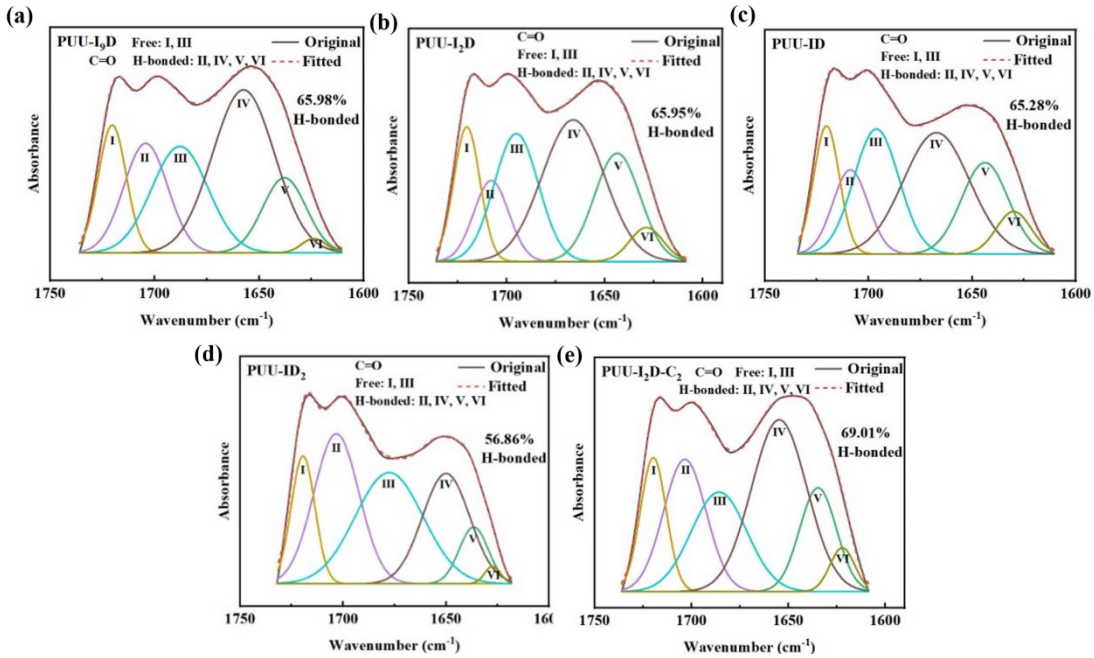

Figure S4 Carbonyl stretching regions of a) PUU-I_9D, b) PUU-I_2D, c) PUU-ID, d) PUU-ID_2, and e) PTUU-C_2.

Hydrogen-Bonding Analysis Degrees of hydrogen bonding obtained from curve-fitting of the C=O region are listed in Tables S4–S8.

Table S4. The degree of H-bonded of PUU-I_9D

PUU-I_9D		**Wavenumber (cm^{-1})**	**Area (%)**
υ(C=O) urethane amide	**Free**	I(1720)	12.63
	H-bonded(ordered)	II(1704)	17.13
υ(C=O) urea amide	**Free**	III(1687)	21.39
	H-bonded(disordered)	IV(1657)	36.07
	H-bonded(ordered)	V(1637)	11.55
υ(C=O) amide	**H-bonded(ordered)**	VI(1623)	1.23

PUU-I_9D		Wavenumber (cm^{-1})	Area (%)
Total	**degree of H-bonded**		65.98

Table S5. The degree of H-bonded of PUU-I_2D

PUU-I_2D		Wavenumber (cm^{-1})	Area (%)
υ(C=O) urethane amide	**Free**	I(1720)	12.98
	H-bonded(ordered)	II(1707)	10.52
υ(C=O) urea amide	**Free**	III(1695)	21.07
	H-bonded(disordered)	IV(1666)	32.84
	H-bonded(ordered)	V(1643)	18.39
υ(C=O) amide	**H-bonded(ordered)**	VI(1628)	4.20
Total	**degree of H-bonded**		65.95

Table S6. The degree of H-bonded of PUU-ID

PUU-ID		Wavenumber (cm^{-1})	Area (%)

υ(C=O) urethane amide	**Free**	I(1720)	12.69
	H-bonded(ordered)	II(1708)	11.58
υ(C=O) urea amide	**Free**	III(1696)	22.03
	H-bonded(disordered)	IV(1667)	31.36
	H-bonded(ordered)	V(1643)	16.63
υ(C=O) amide	**H-bonded(ordered)**	VI(1629)	5.71
Total degree of H-bonded			65.28

Table S7. The degree of H-bonded of PUU-ID_2

PUU-ID_2		**Wavenumber (cm^{-1})**	**Area (%)**
υ(C=O) urethane amide	**Free**	I(1719)	12.25
	H-bonded(ordered)	II(1703)	27.65
υ(C=O) urea amide	**Free**	III(1677)	30.89
	H-bonded(disordered)	IV(1649)	21.38
	H-bonded(ordered)	V(1636)	6.72
υ(C=O) amide	**H-bonded(ordered)**	VI(1627)	1.11
Total degree of H-bonded			56.86

Table S8. The degree of H-bonded of PTUU-C_2

PTUU-C_2		**Wavenumber (cm^{-1})**	**Area (%)**

υ(C=O) urethane amide	**Free**	I(1719)	11.91
	H-bonded(ordered)	II(1703)	19.41
υ(C=O) urea amide	**Free**	III(1685)	19.08
	H-bonded(disordered)	IV(1654)	32.80
	H-bonded(ordered)	V(1634)	13.11
υ(C=O) amide	**H-bonded(ordered)**	VI(1622)	3.69
Total degree of H-bonded			69.01

The toughness and Young's modulus of the elastomer series in Figure 2d are summarized in Table S9. Young's modulus was obtained by linear fitting of the elastic deformation region in the stress–strain curves of the elastomers.

Table S9. Toughness and Young's Modulus of PUU and PTUU Elastomers

Sample	Toughness (MJ m^{-3})	Young's modulus (MPa)
PUU-I_9D	206.55	8.22
PUU-I_2D	251.10	6.42
PUU-ID	188.65	4.99
PUU-ID_2	163.73	4.85
PUU-ID_9	107.96	3.80
PTUU-C_1	270.10	6.98
PTUU-C_2	286.99	7.34
PTUU-C_3	226.21	6.77

Cyclic Tensile Test Ten successive load–unload cycles at 50 %, 100 % and 300 % strain are

shown in Fig. S5.

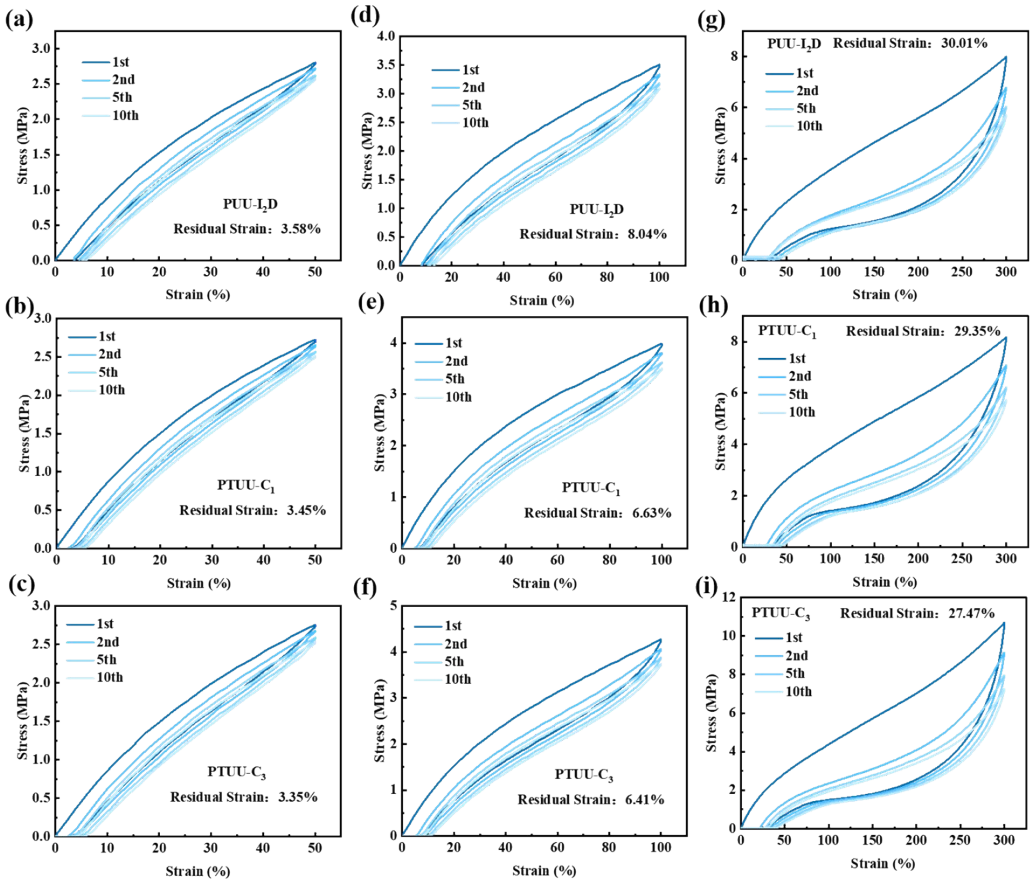

Figure S5. Continuous cyclic tensile curves of (a) PUU-I_2D, (b) PTUU-C_1, and(c) PTUU-C_3 at 50% strain; Continuous cyclic tensile curves of (d) PUU-I_2D, (e) PTUU-$C_1$and(f) PTUU-C_3 at 100% strain; Continuous cyclic tensile curves of (g) PUU-I_2D, (h) PTUU-$C_1$and (i) PTUU-C_3 at 300% strain

Notch Fracture Test Photographs of notched specimens during extension are provided in Fig. S6.

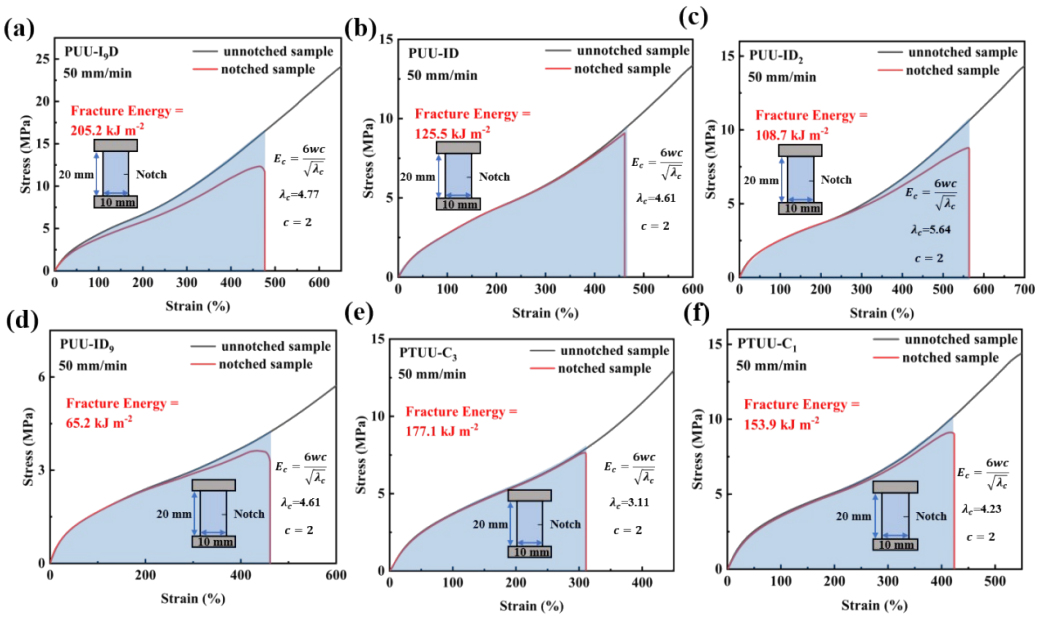

Figure S6. Stress-strain curves of PUU and PTUU elastomers with notch and without notch: (a) PUU-I_9D, (b) PUU-ID, (c) PUU-ID_2, (d) PUU-ID_9, (e) PUU-C_1 and (f) PTUU-C_2

The DMT modulus distribution curves of PUU and PTUU-C_2 are shown in Fig. S7.

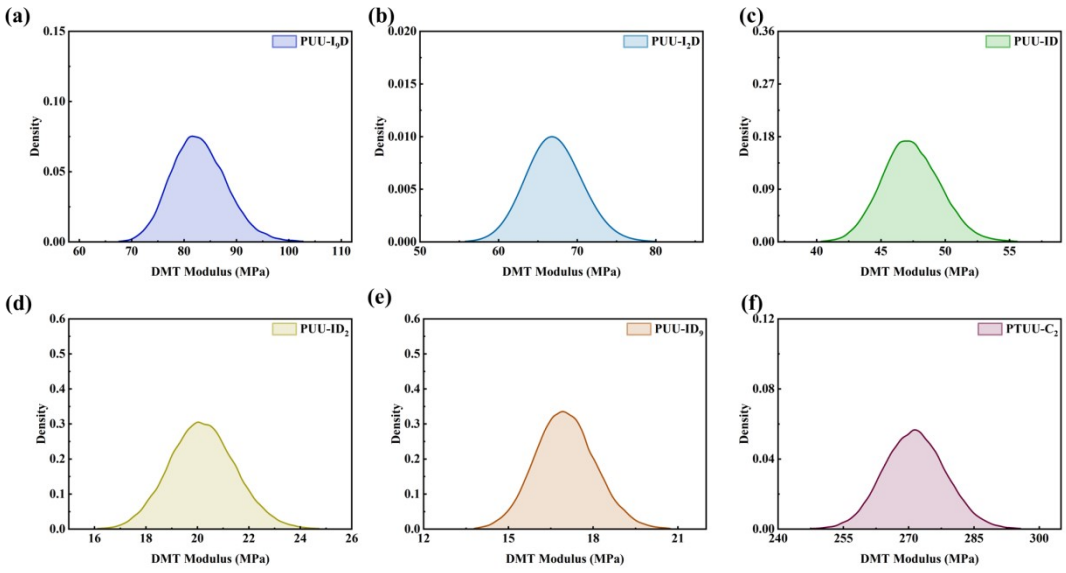

Figure S7.DMT Modulus statistic curve of (a) PUU-I_9D, (b) PUU-I_2D, (c) PUU-ID, (d) PUU-ID_2, (e) PUU-ID_9 and (f) PTUU-C_2

Water Absorption Water-uptake curves recorded over 168 h are displayed in Fig. S8.

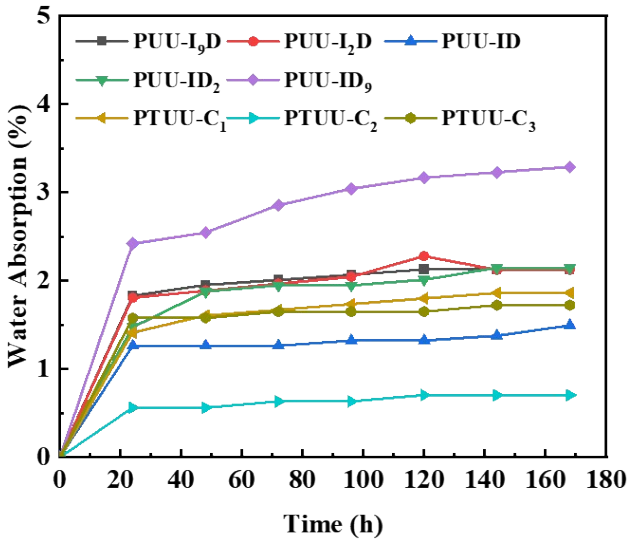

Figure S8. Water absorption of PUU and PTUU elastomers

Periodicity calculation results of hard segment microdomains are shown in Table S10.

Table S10. Hard segment periodicity of PUU-I_9D, PUU-I_2D, PUU-ID and PTUU-C_2

Sample	Periodicity(d)/nm
PUU-I_9D	9.99
PUU-I_2D	9.47
PUU-ID	9.47
PTUU--C_2	10.39

Detailed data of the thermogravimetric analysis are recorded in Table S11.

Table S11. Thermal decomposition temperature of PUU and PTUU elastomers

Sample	Decomposition Temperature(T_5)/℃
PUU-I_9D	315.0
PUU-I_2D	315.2
PUU-ID	311.5
PUU-ID_2	305.0
PUU-ID_9	305.5
PTUU-C_1	296.7
PTUU-C_2	305.1
PTUU-C_3	304.6

Optical Properties Transmittance, haze and refractive-index data are collected in Fig. S9 and Tables S12 and S13.

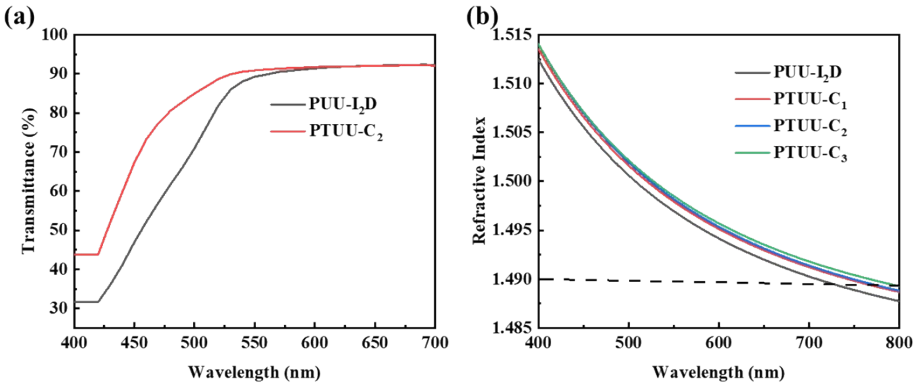

Figure S9. (a) Transmittance of PUU-I_2D and PTUU-C_2 at wavelength from 400 ~ 700 nm; (b) Curve of refractive index of PUU-I_2D and PTUU with wavelength

Table S12. Average transmittance and average haze of PUU-I_2D and PTUU-C_2

Sample	Average transmittance (%)	Average haze (%)
PUU-I_2D	86.04	1.77
PTUU-C_2	89.69	1.23

Table S13. Refractive index of PUU-I_2D and PTUU elastomers at three different wavelengths

Sample	454.7nm	636.85nm	786.2nm
PUU-I_2D	1.5051	1.4923	1.4882
PTUU-C_1	1.5061	1.4933	1.4891
PTUU-C_2	1.5065	1.4934	1.4893
PTUU-C_3	1.5066	1.494	1.4896

Chemical Recycling ^{1}H NMR and FTIR spectra of the recycled thiol-terminated polymer are given in Fig. S10.

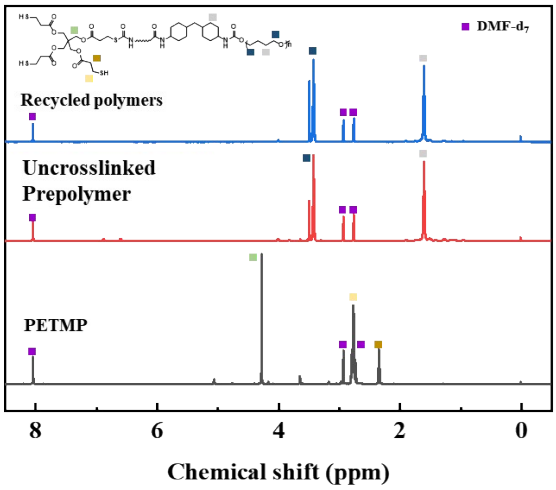

Figure S10.^{1}H NMR spectrum of PETMP, pre-crosslinking(PUU-I_2D) and recycled polymers

Testing Methods (Detailed)

Fourier Transform Infrared (FTIR) Spectroscopy FTIR spectra were recorded on a Bruker VERTEX 70v spectrometer at room temperature. Samples were dissolved in DMAc and drop-cast onto KBr pellets. After drying under reduced pressure, the pellets were measured in transmission mode. Spectra were collected from 4000 to 500 cm^{-1} with a resolution of 2 cm^{-1} and 32 scans.

Tensile Testing Uniaxial tensile tests were performed on an Instron 5966 universal testing machine at 25 °C. Dumb-bell specimens (effective gauge 15 mm × 2 mm × 1 mm) were cut from solvent-cast films and stretched at 50 mm min^{-1} until fracture. Tensile strength, elongation at break and toughness (integral under the stress–strain curve) were averaged over five specimens.

Notch Fracture Energy Single-edge-notched samples (20 mm × 10 mm × 1 mm, notch depth 2 mm) were stretched at 50 mm min^{-1}. The fracture energy (Ec) was calculated using the Greensmith equation: $Ec = 6\omega c / \sqrt{\lambda c}$, where ω is the strain-energy density of the un-notched sample at the elongation of fracture (λc) of the notched specimen.

Dynamic Mechanical Analysis (DMA) DMA was carried out on a TA Q800 analyser in

tension mode. Specimens (10 mm × 6 mm × 1 mm) were heated from −100 to 100 °C at 3 °C min^{-1} under 1 Hz frequency. Storage modulus (E′) and loss factor (tan δ) were recorded.

Self-Healing Test Film strips were cut through ≥80 % of their thickness with a scalpel. The two halves were immediately re-contacted and placed in a convection oven at 100 °C for 48 h without external pressure. Healing efficiency η = (σ_healed / σ_original) × 100 % was determined from tensile tests (five repeats).

Atomic Force Microscopy (AFM) Surface morphology and modulus were mapped on a Bruker Icon microscope in PeakForce QNM mode. Scans (5 × 5 μm^2) were acquired at 0.5 Hz with a silicon tip (spring constant ≈0.4 N m^{-1}). DMT modulus histograms were extracted using NanoScope Analysis.

Small-Angle X-ray Scattering (SAXS) SAXS patterns were collected on a Xenocs Xeuss 2.0 system (Cu Kα, λ = 1.54189 Å, sample-to-detector 1188 mm). Films were exposed for 300 s and azimuthally integrated to obtain one-dimensional profiles. Hard-segment periodicity d was calculated from the peak maximum q* via $d = 2\pi / q^*$.

X-ray Diffraction (XRD) Wide-angle patterns were recorded on a PANalytical X'Pert Pro MRD diffractometer (Cu Kα) from 5 to 60° 2θ with a 0.033° step and 10 s per step.

UV–Vis Spectroscopy Absorption spectra were measured on a Shimadzu UV-2600i spectrophotometer. Thin films spin-coated on quartz slides were scanned from 200 to 800 nm at 1 nm intervals.

Fluorescence Spectroscopy Photoluminescence was recorded on a HORIBA FluoroMax Plus (λex 254 nm, slits 5 nm) or an Edinburgh FLS1000 (λex 350 nm, slits 4 nm). Emission was collected from 274 to 540 nm or 370 to 680 nm, respectively, with 1 nm steps.

Thermogravimetric Analysis (TGA) TGA was performed on a Netzsch TG209F3 under

nitrogen (50 mL min^{-1}). Samples (3–5 mg) were heated from 35 to 600 °C at 10 °C min^{-1}. The temperature at 5 % mass loss (T_5) was used as the decomposition onset.

Cyclic Tensile Test Load–unload cycles (10 consecutive) were performed at 50 mm min^{-1} with maximum strains of 50 %, 100 % or 300 %. After the 10th cycle, samples were rested for 10 min and then pulled again to evaluate recovery.

Stress Relaxation A TA Q800 analyser applied 1 % tensile strain at 100 °C. The decay of stress was recorded for 60 min and normalised by the initial stress σ_0.

Water Absorption Rectangular films (20 × 10 × 1 mm) were immersed in de-ionised water at 25 °C. Mass was recorded every 24 h for 168 h after gently wiping off surface water. Water uptake (%) = $(m_t - m_0) / m_0 \times 100$. After immersion, samples were dried at 80 °C for 24 h and re-tested in tension.

Swelling and Gel Content ~0.5 g films were immersed in acetone at 25 °C for 72 h to reach equilibrium. After blotting, the swollen mass m_1 and dried mass m_2 (80 °C, 2 h) were recorded.

$$\text{Swelling ratio } S = (m_1 - m_0) / m_0 \times 100\ \%$$

$$\text{Gel content } G = m_2 / m_0 \times 100\ \%$$

Thermal-Oxidative Aging Following GB/T 3512-2014, films were aged in a forced-air oven at 110 °C for 168 h. Tensile properties before and after aging were compared.

Refractive Index A Metricon 2010/M prism coupler was used at 454.7, 636.85 and 786.2 nm. Films (15 × 15 × 1 mm) were pressed against the prism; the critical angle was converted to refractive index using the instrument software.

^{1}H NMR Spectroscopy Spectra were acquired on a Bruker AVANCE III HD 600 MHz spectrometer at 25 °C. Approximately 10 mg of polymer was dissolved in 0.6 mL DMF-d_7. Sixteen scans were accumulated with a 5 mm PABBO probe.